

1 **Targeting riboswitches with synthetic small RNAs for metabolic engineering**

2

3 Milca Rachel da Costa Ribeiro Lins^{1*}, Laura Araujo da Silva Amorim^{1*}, Graciely Gomes

4 Correa¹, Bruno Willian Picão¹, Matthias Mack², Marcel Otávio Cerri¹, Danielle Biscaro

5 Pedrolli^{1†}

6

7 ¹Universidade Estadual Paulista (UNESP), School of Pharmaceutical Sciences,

8 Department of Bioprocess Engineering and Biotechnology, Rodovia Araraquara-Jau

9 km1, 14800-903 Araraquara, Brazil

10 ²Mannheim University of Applied Sciences, Institute for Technical Microbiology, Paul-

11 Wittsack-Str. 10, 68163 Mannheim, Germany

12

13 *Contributed equally as first author

14 †Corresponding author:

15 Danielle B. Pedrolli, e-mail: danielle.pedrolli@unesp.br

16

17 **Abstract**

18 Our growing knowledge of the diversity of non-coding RNAs in natural systems and our
19 deepening knowledge of RNA folding and function have fomented the rational design of
20 RNA regulators. Based on that knowledge, we designed and implemented a small RNA
21 (sRNA) tool to target bacterial riboswitches and activate gene expression. The synthetic
22 sRNA is suitable for regulation of gene expression both in cell-free and in cellular
23 systems. It targets riboswitches to promote the antitermination folding regardless the
24 cognate metabolite concentration. Therefore, it prevents transcription termination
25 increasing gene expression up to 103-fold. We successfully used sRNA arrays for
26 multiplex targeting of riboswitches. Finally, we used the synthetic sRNA to engineer an
27 improved riboflavin producer strain. The easiness to design and construct, and the fact
28 that the riboswitch-targeting sRNA works as a single genome copy, make it an attractive
29 tool for engineering industrial metabolite-producing strains.

30

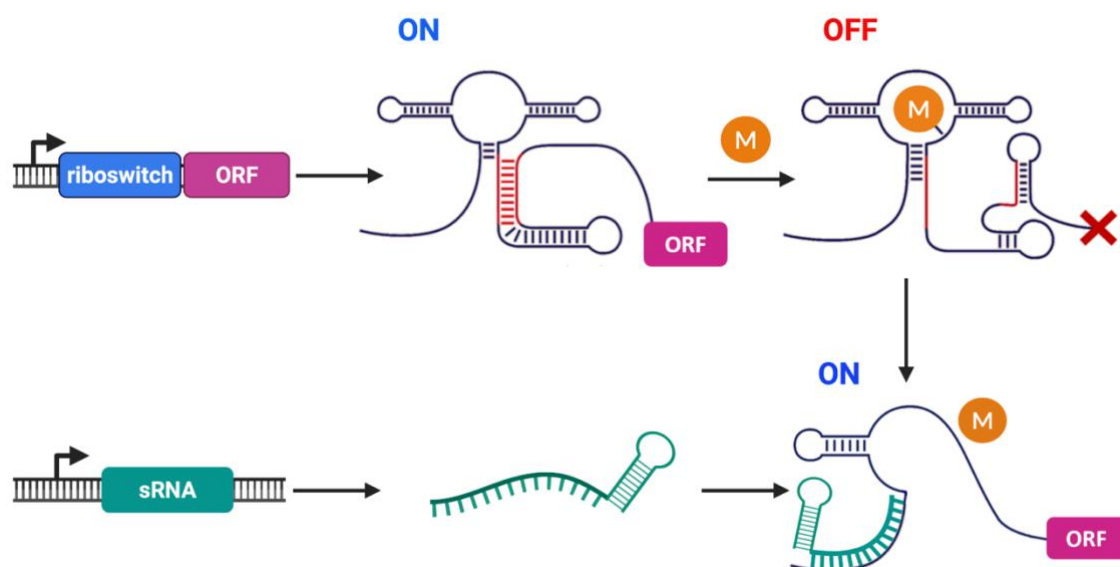
31

32 **Keywords:** small RNA, non-coding RNA, riboswitch, *Bacillus subtilis*, synthetic biology,
33 riboflavin.

34

35 **Graphical Abstract**

36



37

38

39 1. Introduction

40 RNAs are important regulatory tools in the synthetic biology toolbox for controlling gene
41 expression and constructing synthetic gene networks (Chappell et al., 2015b; Leistra et
42 al., 2019). Among all regulatory RNAs, trans-acting antisense small RNAs (sRNAs) are
43 particularly attractive to engineer due to their simplicity, fast response to external signals,
44 and usefulness for fine-tuning of gene expression (Shimoni et al., 2007). The simplicity
45 of the RNA sequence and the predictability of RNA folding has powered the development
46 of sRNA rational design to tune gene expression. Moreover, the specificity of base-
47 pairing and easiness to construct make sRNA an ideal tool for circuit design and
48 multiplex control (Kelly et al., 2018; Noh et al., 2017). Compared to protein-based
49 regulation, sRNAs offer multiple options for the design of orthogonal control with minimal
50 or no metabolic burden associated. Therefore, synthetic sRNAs are simple and versatile
51 tools to regulate gene expression and engineer metabolic pathways.

52 Synthetic sRNAs have been mostly used as antisense RNAs to block the access of the
53 ribosome to the mRNA and prevent translation in *E. coli*. sRNA-mediated knockdown
54 has been successfully used to fine-tune gene expression and develop *E. coli*
55 superproducers of industrially relevant compounds such as tyrosine, proline, cadaverine,
56 putrescine, 4-hydroxycoumarin, resveratrol, and naringenin (Na et al., 2013; Noh et al.,
57 2017; Yang et al., 2015). The strategy has been once used in *B. subtilis* to engineer a
58 N-acetylglucosamine producer strain (Liu et al., 2014). Now, we expand the functionality
59 of sRNAs to target riboswitches and activate gene expression at the transcription level.
60 Riboswitches play an important role in the regulation of gene expression in bacteria. In
61 *B. subtilis* there are 41 identified riboswitches that regulate ~2% of all genes, many of
62 them related to the biosynthesis of industrially relevant compounds (Kalvari et al., 2021;
63 Mandal et al., 2003). Bacterial riboswitches ultimately regulate the levels of metabolites
64 in the cell through the control of biosynthesis and/or transport processes (Mandal et al.,
65 2003; Mars et al., 2016). Although tempting, deletion of riboswitches aiming to create
66 constitutive expression leads to severe decrease in gene expression (Boumezbeur et

67 al., 2020; Shi et al., 2014). Alternatively, we propose the use of riboswitch-targeting
68 sRNAs for dynamic control of gene expression.

69 Riboswitches that bind organic small molecules, such as purines, vitamins, and amino
70 acids, keep the cell homeostasis preventing unneeded accumulation of cellular
71 compounds. In *B. subtilis* and other bacteria the control exerted by riboswitches is most
72 pronounced during the exponential growth phase when the intense cell metabolism
73 favors biosynthetic processes (Lins et al., 2021; Pedrolli et al., 2015, 2012). The
74 developed riboswitch-targeting sRNAs act at that time point, interfering with the
75 riboswitch aptamer folding, preventing transcription termination, and stabilizing the
76 mRNA, which leads to metabolite accumulation.

77

78 **2. Materials and methods**

79 **2.1. sRNA design analysis *in silico***

80 The synthetic RNAs were designed for each riboswitch using the RiboMaker software
81 (Rodrigo and Jaramillo, 2014; Rostain et al., 2015). The thermodynamic properties of the
82 sRNAs were evaluated using the NUPACK Web Application (Zadeh et al., 2011).

83

84 **2.2. Plasmids and other DNA sequences**

85 Plasmids for riboswitch control of gene expression have been constructed previously
86 (Lins et al., 2021). Shortly, for *in vitro* gene expression each riboswitch was cloned
87 between the *E. coli ribB* promoter and the firefly luciferase gene (*luc*) to generate plasmid
88 series P_{ribB}-riboswitch-*luc*. For *in vivo* gene expression, expression each riboswitch was
89 cloned between the P_{srfA} promoter and the *luxABCDE* operon to generate the plasmid
90 series pBS3C-riboswitch-*lux*. The plasmids integrate at the *sacA* locus in *B. subtilis*.

91 The synthetic sRNAs were purchased as oligonucleotides forward and reverse strands,
92 annealed, and cloned into the pBS2E plasmid (Radeck et al., 2013) together with the
93 P_{grac} promoter to generate the plasmid series pBS2E-P_{grac}-sRNA. The plasmids integrate

94 at the *lacA* locus in *B. subtilis*. The P_{grac}-sRNA-*purE*-broccoli sequence was cloned into
95 the pBS1C plasmid (Radeck et al., 2013) and integrated at the *amyE* locus in *B. subtilis*.
96 The sRNA operon was assembled from 28 semi-complementary oligonucleotides
97 designed with GeneDesign (Richardson et al., 2006). Four building blocks were
98 generated by PCR gene synthesis (Rouillard et al., 2004). The four blocks were then
99 assembled using Overlap Extension PCR. Lists of plasmids and strains used are
100 provided in the supplementary tables S1 e S2.

101

102 **2.3. *In vitro* transcription**

103 RNAs transcripts were generated by *in vitro* transcription using the RiboMAX™ Large
104 Scale RNA Production Systems (Promega). Annealed oligonucleotides forward and
105 reverse containing the T7 promoter and the sRNA were used as template. Reactions
106 were incubated at 37°C overnight. Reaction inactivation was performed at 70°C for 20
107 min. To eliminate the template, all samples were treated with RQ1 RNase-Free DNase
108 (Promega) for 1 hour at 37°C. Samples were then precipitated with ethanol and
109 resuspended in RNase-free water.

110

111 **2.4. *In vitro* gene expression**

112 The regulatory activity of the sRNAs was accessed by *in vitro* gene expression reaction
113 according to Lins et al. (Lins et al., 2021). Each P_{ribB}-riboswitch-*luc* plasmid was extracted
114 from overnight grown *E. coli* with a miniprep kit (PureYield™ Plasmid Miniprep System,
115 Promega) and purified using ethanol precipitation. Plasmids were resuspended in
116 RNase-free water and used as templates for *in vitro* gene expression (*E. coli* S30 Extract
117 System for Circular DNA, Promega). Reactions were set up by adding 1 µL of 0.25 mM
118 amino acid mix, 4 µL of S30 Premix, 3 µL of S30 Extract, 1 µL of 50 µM ligand (guanine,
119 adenine or FMN; Merck), 1 µL of transcribed sRNA (30 ng µL⁻¹), and 1 µL of plasmid (5
120 ng µL⁻¹). The reaction mixture was incubated at 30°C for 20 min, and 90 µL of 1% (m/v)

121 bovine serum albumin was added to stop the reactions. Each treatment was performed
122 in triplicate.

123 In order to quantify the luciferase activity, 10 μ L of stopped reactions were added to 50
124 μ L of luciferase substrate solution (Luciferase Assay System kit, Promega) in a 96-well
125 white flat bottom microplate. Luminescence readings were taken on a microplate reader
126 (Tecan Infinite 200 Pro, Switzerland) set with 1,000 ms for integration time at 26°C.

127

128 **2.5. Bacterial strains and media**

129 *E. coli* Top10 was used for cloning and propagation of plasmids. It was aerobically
130 cultivated at 37°C in Lysogeny Broth (LB) enriched with antibiotics when needed. *B.*
131 *subtilis* 168, *B. subtilis* riboflavin producer (BsRF), and *B. subtilis* Ai (BsAi) (Correa et al.,
132 2020) were used as chassis for the experiments as indicated in the main text. All *B.*
133 *subtilis* strains were aerobically cultivated in LB for all experiments regarding
134 bioluminescence measurements. A high sugar complex medium was used for riboflavin
135 production in all scales (PW medium: 40 g L⁻¹ sucrose, 1 g L⁻¹ yeast extract, 25 g L⁻¹
136 NaNO₃, 0.333 g L⁻¹, KH₂PO₄, 1 g L⁻¹ Na₂HPO₄·12H₂O, 0.15 g L⁻¹ MgSO₄·7H₂O, 7.5 mg
137 L⁻¹, CaCl₂, 6 mg L⁻¹ MnSO₄·H₂O, 6 mg L⁻¹, FeSO₄ 7H₂O, pH 7.0). *B. subtilis* culture
138 medium was enriched with chloramphenicol (5 μ g mL⁻¹) and/or erythromycin (1 μ g mL⁻¹)
139 when needed.

140

141 **2.6. Bioluminescence and growth measurements**

142 Bioluminescence measurements from growing *B. subtilis* were carried out in white 96-
143 well microplates with optically clear bottoms. Culture density was monitored by
144 absorbance measurements at 600 nm (OD₆₀₀) taken from the same transparent bottom
145 microplates. Plates were incubated at 37°C and orbital shaking at 143 rpm.
146 Measurements were performed every 10 min for five hours in the microplate reader
147 (Tecan Infinite 200 Pro). All experiments were performed with three biological replicates.

148

149 **2.7. Broccoli-DFHBI fluorescence measurements**

150 The RNA-Broccoli (Filonov et al., 2014) was fused to the *purE*-sRNA under control of the
151 P_{grac} for detection of transcripts in *B. subtilis*. After induction with IPTG, samples were
152 withdrawn and incubated for 30 min with the fluorophore DFHBI. Then, fluorescence
153 measurements were taken in a 96-well black microplate with the microplate reader set
154 at 472 nm for excitation and 507 nm for emission.

155

156 **2.8. Test tube and Erlenmeyer scale cultivation**

157 *B. subtilis* cultivation was performed in 16 x 220 mm (d x L) test tubes filled with 5 mL
158 culture medium and incubated at 37°C and 220 rpm. *B. subtilis* culture was also carried
159 out in 250 mL baffled Erlenmeyer flasks filled with 20 mL culture medium and incubated
160 at 37°C and 150 rpm. Samples were periodically withdrawn for absorbance
161 measurements at 600 nm (OD_{600}) in a microplate reader (Tecan Infinite 200 Pro,
162 Switzerland), and for riboflavin quantification by HPLC. All experiments were performed
163 with three biological replicates.

164

165 **2.9. Bioreactor scale cultivation**

166 A stirred batch was carried out at 37°C, 0,5 vvm air supply, and pH controlled at 7.0 ± 0.1 .
167 The bioreactor 7L tank was filled with 5L of PW medium supplemented with 80 g.L^{-1}
168 sucrose. After inoculation, samples were withdrawn periodically for sucrose, riboflavin,
169 and biomass quantification. Biomass quantification was accessed as dry weight per liter.

170

171 **2.10. Riboflavin and sucrose quantification**

172 Samples withdrawn from cultures were centrifuged at 16,000 xg for 30 min for
173 supernatant recovery. Trichloroacetic acid 1% (v/v) was added to the supernatant to
174 precipitate proteins. The resulting samples were centrifuged at 16,000 xg for 20 min. The
175 supernatant was then filtered using a hydrophilic PTFE 0.20 μm membrane, and the

176 filtrate was used for analysis by high-performance liquid chromatography (HPLC;
177 Shimadzu LC-20AD equipped with a SPD-M20A photodiode detector).

178 Riboflavin was analyzed using a 50 x 3 mm Poroshell 120 EC-C18 column (Agilent
179 Technologies) in 82% solvent A (20 mM formic acid, 20 mM ammonium formate) and
180 18% solvent B (methanol) as mobile phase at 0.5 mL/min, in isothermal mode at 30°C.
181 Detection was performed at 445 nm. Commercial riboflavin (Merck) was used as
182 standard for calibration.

183 Sucrose was analyzed using a HPX-87P column (Aminex) in ultrapure water as mobile
184 phase at 0.6 mL/min, in isothermal mode at 80°C.

185

186 **2.11. Statistical analysis**

187 Analysis of variance (ANOVA) and Tukey test were performed using the Minitab software
188 (version 18), to compare the averages and observe the significance of the results.

189

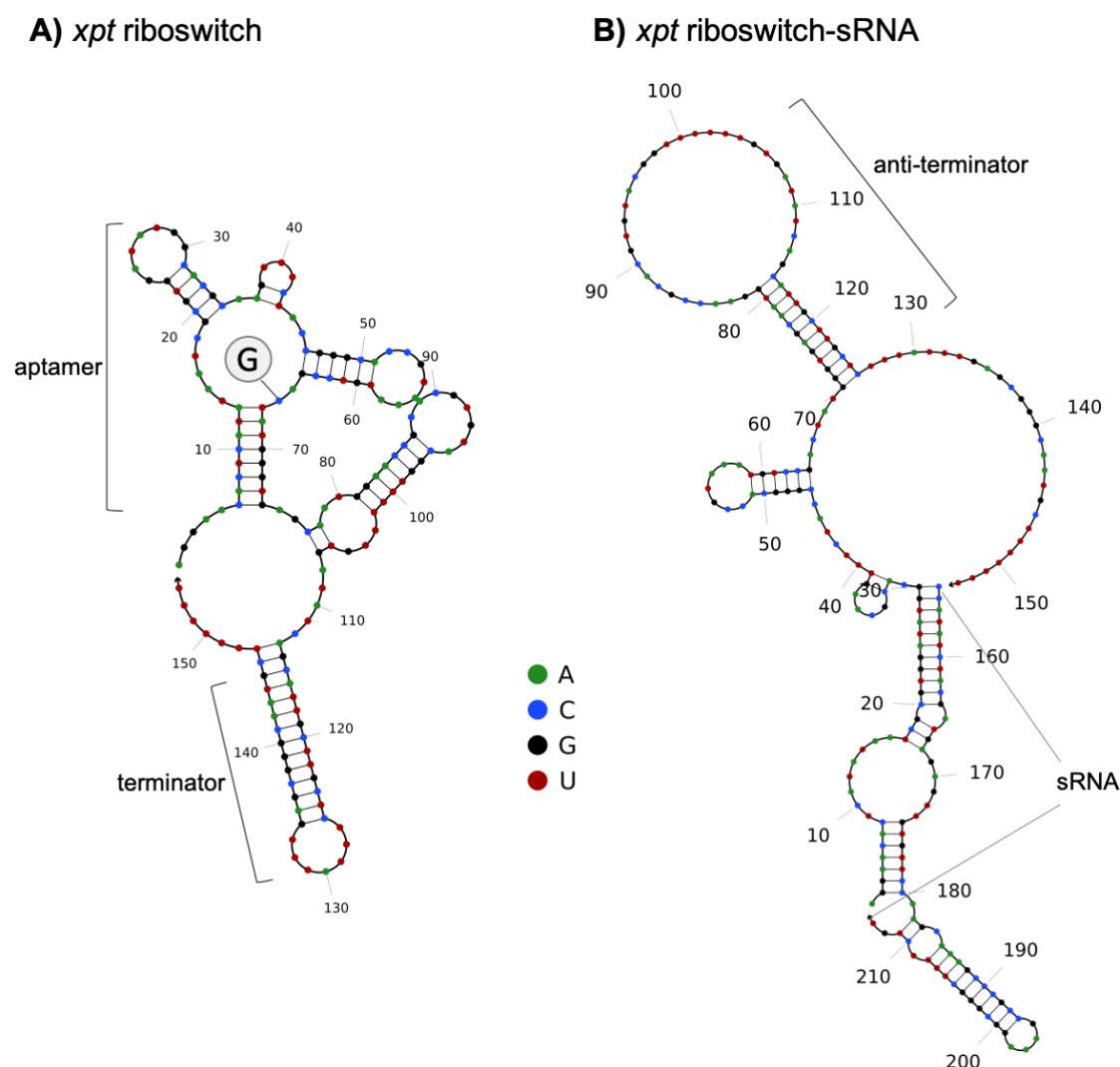
190 **3. Results**

191 **3.1. Designing small regulatory RNAs to target riboswitches**

192 We have chosen the well-studied purine riboswitches *purE*, *xpt*, *nupG*, and *pbuE*, and
193 the flavin riboswitch *ribDG* of *B. subtilis* as targets for sRNA design. Together they control
194 the purine uptake and synthesis and the riboflavin synthesis through premature
195 transcription termination (Johansen et al., 2003; Lins et al., 2021; Mandal et al., 2003).

196 The sRNA was designed to target each riboswitch in order to prevent folding into the
197 OFF structure that leads to premature transcription termination (Figure 1). The sRNA
198 was designed to counteract the riboswitch activity and keep gene expression ON even
199 at high cognate metabolite concentration by promoting the anti-terminator formation
200 even when it shouldn't. Target sequences in the aptamers have been previously
201 identified through point mutation as crucial for the OFF state folding (Mandal and
202 Breaker, 2004; Marcano-Velázquez and Batey, 2015; Mironov et al., 2002). sRNA
203 sequences targeting each riboswitch were generated using RiboMaker (Rodrigo and

204 Jaramillo, 2014) and analyzed using NUPACK (Zadeh et al., 2011). The best sRNAs
205 were selected based on the hybridization free energy (lower than -18 Kcal/mol), the
206 seed-based free energy, ensemble defect (lower than 10%), and the complex
207 representation at equilibrium (Rostain et al., 2015). One sRNA targeting each riboswitch
208 was selected for construction and test (Table S3).
209

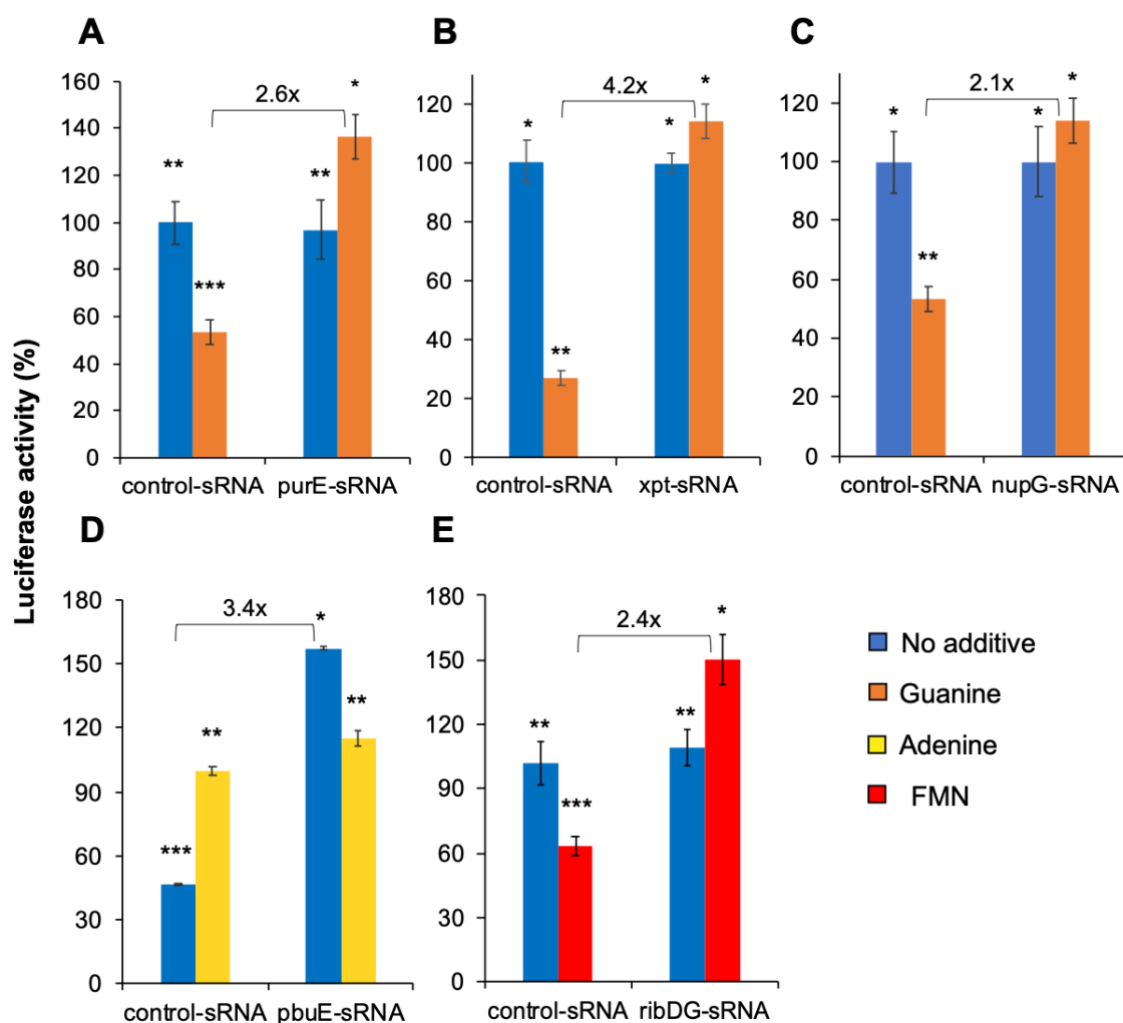


210
211 **Figure 1.** Riboswitch-sRNA pairing. (A) sequence and structure of the *xpt* riboswitch bound to
212 guanine. (B) sequence and structure of the *xpt* riboswitch paired with the *xpt*-sRNA. sRNA pairing
213 with the riboswitch nucleotides 2-30 results in an alternative folding, that leads to the formation of
214 the anti-terminator stem loop through base-pairing between nucleotides 70-81 and 115-126. All
215 riboswitch-targeting sRNAs were designed to target the aptamer sequence in order to promote
216 the anti-terminator formation. Figure generated using NUPACK Web Application.

217 **3.2. Synthetic sRNAs counteract riboswitches' control of gene expression *in***
218 ***vitro***

219 In order to evaluate the specific ability of each synthetic sRNA to bind its target riboswitch
220 and activate gene expression, we set an *in vitro* gene expression reaction which has
221 been validated for riboswitch characterization (Lins et al., 2021). Expression of the firefly
222 luciferase gene under the control of each riboswitch was evaluated in the presence of
223 the sRNA and the cognate metabolite (guanine, adenine, or FMN). Each sRNA was
224 previously transcribed *in vitro* and purified. All sRNAs were able to completely counteract
225 their target riboswitch's regulatory activity turning ON gene expression when it was
226 supposed to be OFF (Figure 2). The activation fold ranged from 2.1 to 4.2. Interestingly,
227 the sRNAs *purE*, *pbuE*, and *ribDG* activated gene expression to levels above the
228 riboswitches' ON state (Figures 2A, D, and E). The sRNA effect on the riboswitch was
229 compared to control-sRNAs, which are riboswitch-targeting sRNAs tested against non-
230 target riboswitches.

231



232

233

234 **Figure 2.** sRNA activity and specificity assayed by *in vitro* expression of the firefly luciferase gene.

235 (A) *purE* riboswitch. (B) *xpt* riboswitch. (C) *nupG* riboswitch. (D) *pbuE* riboswitch. (E) *ribDG*

236 riboswitch. The sRNA effect on the riboswitch was compared to control-sRNAs, which are

237 riboswitch-targeting sRNAs tested against non-target riboswitches. Asterisks identify statistically

238 significant differences ($p < 0.05$). Data are presented as mean \pm SD ($n = 3$). Raw data available

239 in Supplementary Data 1.

240

241 3.3. Synthetic sRNAs are transcribed and functional in the cell

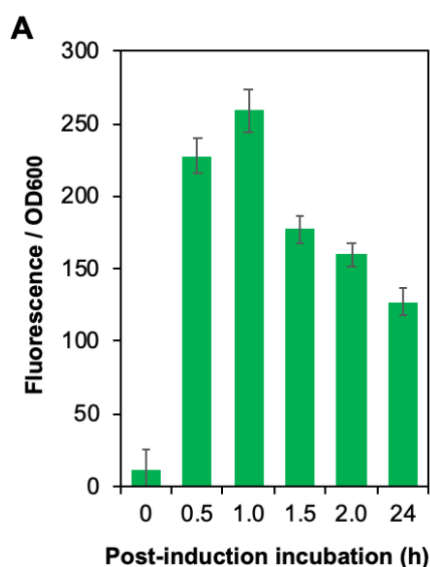
242 After confirming that each synthetic sRNA can specifically counteract the target

243 riboswitch *in vitro*, we moved to *B. subtilis* to verify whether the sRNA could be stably

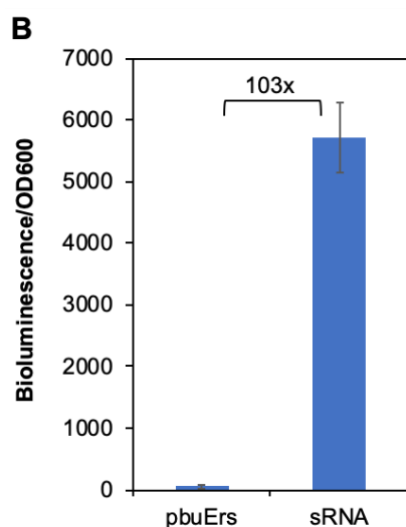
244 transcribed *in vivo*. Therefore, the *purE*-sRNA was fused to the broccoli sequence at the

245 3'-end and integrated as single-copy to the chromosome. Expression of the *purE*-sRNA-

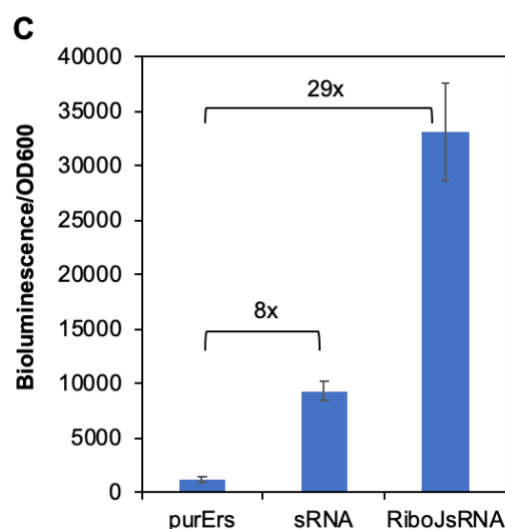
246 broccoli was induced with IPTG in the early-exponential phase, and samples were taken
247 for DFHBI-broccoli fluorescence measurements. A fluorescence peak was detected 1h
248 post-induction and fluorescence was still detectable after 24h (Figure 3A).
249



250



251



252

253 **Figure 3.** sRNA expression and activity assayed in *B. subtilis*. (A) sRNA-broccoli-DFHBI
254 fluorescence. (B) the *lux* operon under control of the *pbuE* riboswitch (pbuErs) and the *pbuE*-
255 sRNA (sRNA) activation effect on the riboswitch. (C) the *lux* operon under control of the *purE*
256 riboswitch (purErs) and the *pbuE*-sRNA (sRNA) and the RiboJ-*purE*-sRNA (RiboJsRNA)
257 activation effect on the riboswitch. Data are presented as mean \pm SD (n = 3). Raw data available
258 in Supplementary Data 2.

259

260 After validating the ability of *B. subtilis* to stably transcribe the sRNA, we constructed a
261 reporter assay to access the sRNA activity *in vivo*. Therefore, the *luxABCDE* operon was
262 used as a reporter under the control of the riboswitches *purE* and *pbuE*. Each riboswitch-
263 *lux* construct was inserted as single-copy at the locus *sacA*, and the corresponding sRNA
264 was integrated at the *lacA* locus in the chromosome. The sRNA transcription was driven
265 by the strong P_{grac} promoter working constitutively (the strain lacks a *lacI* gene). The
266 resulting strains were cultivated in Erlenmeyer flasks filled with LB medium without
267 additives and monitored for bioluminescence for 8h. The *pbuE*-sRNA showed a strong
268 activity activating gene expression up to 103-fold (Figure 3B), much higher than
269 observed *in vitro*. The *purE*-sRNA caused an 8-fold increase in gene expression (Figure
270 3C), which is three times higher than achieved *in vitro*. Although higher than *in vitro*, gene
271 the *purE*-sRNA activating activity *in vivo* is much lower than the activity measured for the
272 *pbuE*-sRNA. We hypothesized that the *purE*-sRNA lower activity could be caused by low
273 RNA stability in the cell. Therefore, we fused it to the RiboJ ribozyme to create the
274 RiboJ*purE*-sRNA. RiboJ greatly improved the sRNA, causing a 29-fold increase in gene
275 expression (Figure 3C). RiboJ is a structured RNA able to self-cleave at the 5'-end that
276 has been used to insulate mRNAs (Lou et al., 2012). Any other structured RNA could
277 have had the same beneficial effect on the sRNA; however, a self-cleaving ribozyme
278 offers the possibility to build an sRNA array for targeting multiple loci (multiplex control).
279 Noteworthy, the sRNAs *pbuE* and RiboJ*purE* improved the strain growth significantly
280 compared to the control strains carrying the riboswitch-controlled *lux* operon but no
281 sRNA (Figure S1). The low-efficient *purE*-sRNA did not cause any change in the strain
282 growth.

283

284 **3.4. Engineering an improved riboflavin producer strain**

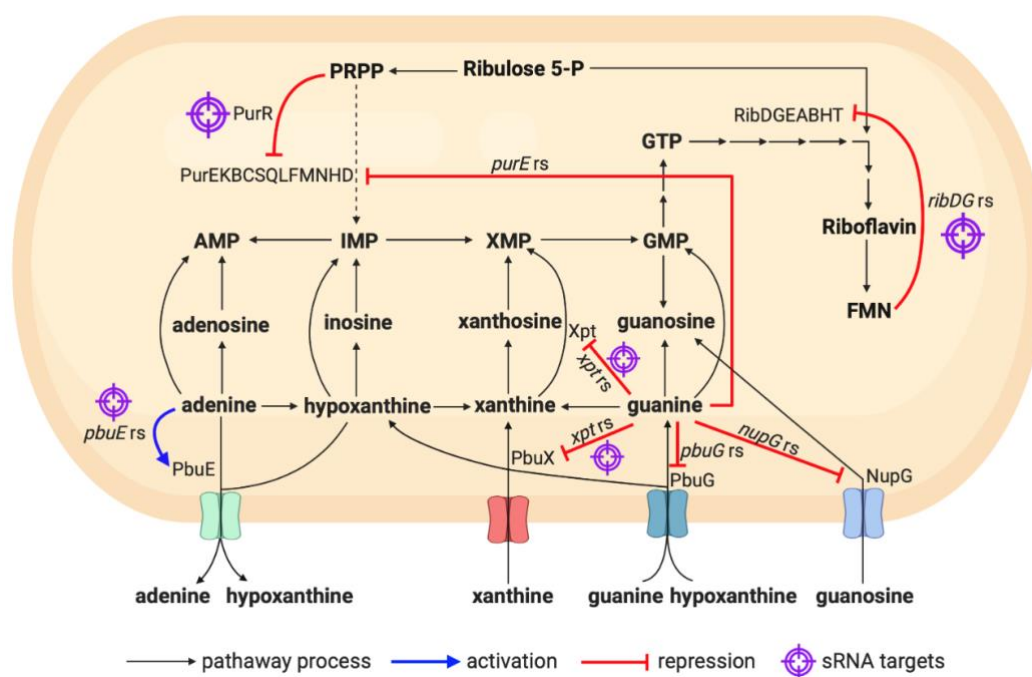
285 Synthetic sRNA has great applicability as a tool to fine-tune gene expression in metabolic
286 pathways. However, it has mostly been used to downregulate gene expression (Liu et

287 al., 2014; Na et al., 2013; Noh et al., 2017; Sun et al., 2019; Yang et al., 2019, 2015). In
288 order to demonstrate the potential of the riboswitch-targeting sRNA for metabolic
289 engineering, we tested the sRNA ability to improve the riboflavin production directly by
290 targeting the *rib* operon, and indirectly by targeting the purine supply (Figure 4). The
291 sRNAs *ribDG*, *purE*, *RiboJpurE*, *xpt*, and *pbuE* were individually inserted into the
292 genome of a riboflavin super-producing strain (BsRF) as single copies. Riboflavin
293 production was first evaluated in test tubes (Figure 5A). Although the sRNAs *purE* and
294 *RiboJpurE* have been previously proved to be functional *in vivo*, they did not improve the
295 riboflavin production. Both target the *pur* operon, which is responsible for the synthesis
296 of inosine monophosphate (IMP) from phosphoribosyl- α -1-pyrophosphate (PRPP). IMP
297 is the precursor for AMP, GMP, and hypoxanthine; therefore, the carbon flux may divert
298 to other routes instead of GTP.

299 The *pbuE* sRNA targets the expression of the adenine exporter PbuE, increasing it.
300 Although the *pbuE* sRNA has proven highly functional using the lux reporter, the strain
301 carrying it produced lower levels of riboflavin (Figure 5A). Increased adenine efflux
302 probably increased the IMP consumption to reset the intracellular adenine concentration,
303 which could cause a reduced flux through GMP synthesis.

304 The sRNAs *xpt* and *ribDG*, on the other hand, were able to increase the riboflavin
305 production by 48% and 30%, respectively. The *xpt* sRNA targets the expression of the
306 *xpt-pbuX* operon. *pbuX* encodes a membrane protein that imports xanthine from the
307 medium. *xpt* encodes a xanthine phosphoribosyl transferase, which converts xanthine to
308 xanthine monophosphate (XMP) (Christiansen et al., 1997). XMP is then converted to
309 GTP, which serves as a direct precursor to riboflavin (Figure 4). The *ribDG* sRNA targets
310 the *ribDGBAHT* operon, which encodes the enzymes directly responsible for riboflavin
311 biosynthesis from GTP and ribulose (Bacher et al., 1993).

312



313

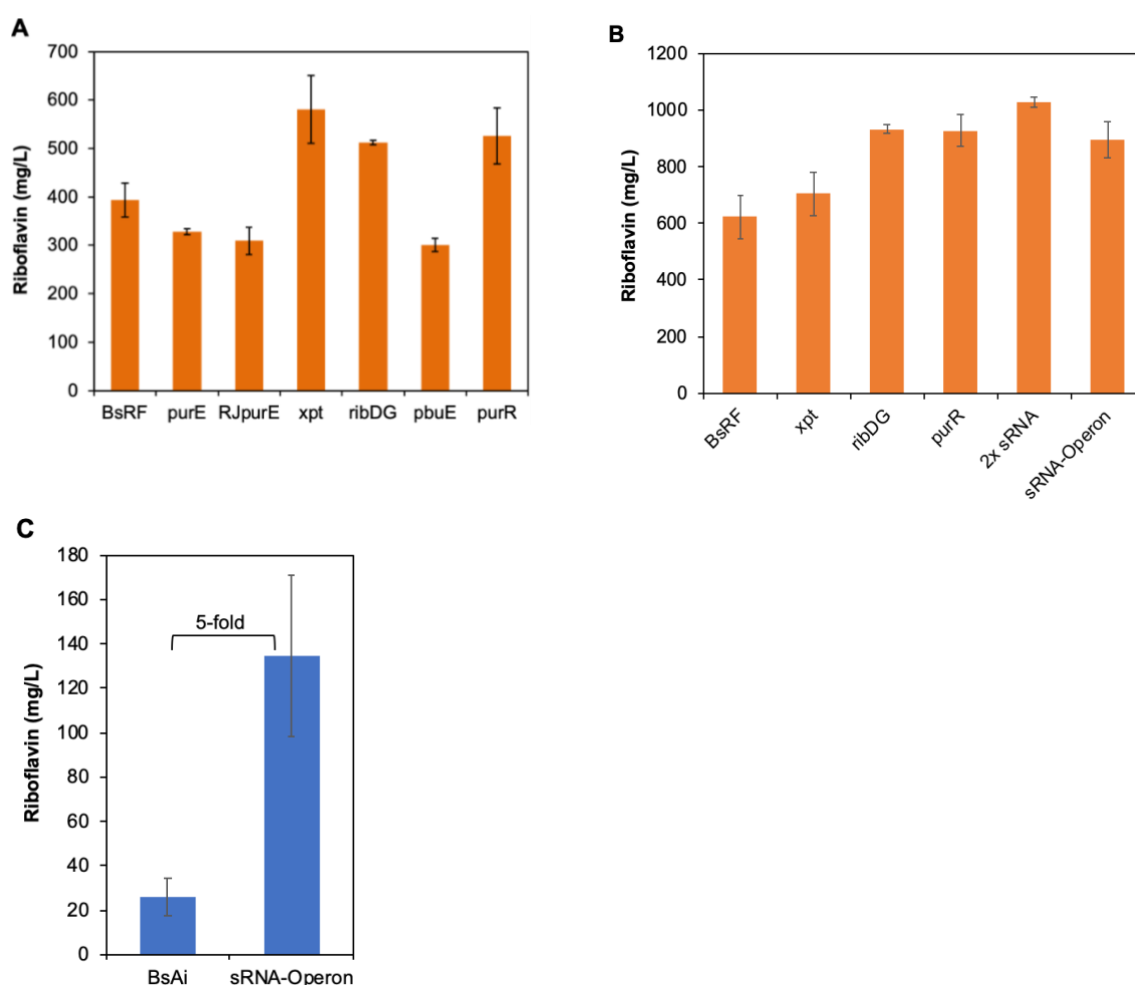
314 **Figure 4.** Metabolic engineering of *B. subtilis* RF (BsRF) for riboflavin production using sRNAs.

315 The riboswitches identified as *purE rs*, *pbuE rs*, *xpt rs*, *pbuG rs*, *nupG rs*, and *ribDG rs* regulate
316 the expression of important genes and operon from the purine and riboflavin metabolism.

317

318 To compare the performance of the designed riboswitch-targeting sRNAs with traditional
319 antisense sRNAs (Liu et al., 2014; Na et al., 2013) we inserted the *purR*-sRNA into the
320 *B. subtilis* chromosome. The latter was designed to pair with the *purR* mRNA from the
321 RBS to the +14 ribonucleotide, thereby blocking translation initiation. The antisense RNA
322 targets the synthesis of PurR, a repressor that blocks transcription initiation of several
323 genes involved in the purine metabolism including the *pur* operon and *xpt-pbuX* (Saxild
324 et al., 2001). The strain carrying the *purR*-sRNA produced 34% more riboflavin than the
325 control (Figure 5A), resembling the *xpt*-sRNA and *ribDG*-sRNA carrying strains.

326



327

328

329 **Figure 5.** Engineering *B. subtilis* with sRNAs for riboflavin production. (A) Test tube cultivation to
 330 evaluate the effect of sRNAs on the riboflavin production. The effect of the sRNAs *purE*, *RiboJ-*
 331 *purE*, *xpt*, *ribDG*, *pbuE*, and *purR* were tested in the BsRF strain. (B) Erlenmeyer cultivation of
 332 the BsRF strains carrying the best sRNAs (*xpt*, *ribDG*, and *purR*) individually, an sRNA array
 333 composed of 2 sRNAs (*ribDG* and *purR*), and an sRNA operon composed of five sRNAs (*purE*,
 334 *xpt*, *ribDG*, *pbuE*, and *purR*). (C) The sRNA operon tested in the *B. subtilis* strain BsAi. Data are
 335 presented as mean \pm SD ($n = 3$). Raw data available in Supplementary Data 3.

336

337 The most promising strains, carrying the sRNAs *xpt*, *ribDG*, and *purR*, were further tested
 338 in Erlenmeyer flasks (Figure 5B). Upscaling resulted in increased riboflavin production
 339 for all tested strains. The highest production was triggered by the sRNAs *ribDG* and *purR*
 340 reaching over 900 mg/L, which is about 50% higher than the control. The *xpt*-sRNA did
 341 not repeat the performance shown on a smaller scale and only slightly increased the

342 riboflavin production, not significantly though. Interestingly, the strain carrying the *xpt*-
343 sRNA grew as poor as the riboflavin super-producing strain (BsRF), whose slow growth
344 has been ascribed to the burden of riboflavin overproduction. However, the two sRNAs
345 that increased the riboflavin production, *ribDG* and *purR*, seem to restore the growth
346 capability of the producer strain reaching cell densities around 2.5-fold higher than BsRF
347 after 40h (Figure S2).

348

349 **3.5. Multiplex sRNA for targeting riboswitches simultaneously**

350 After testing the synthetic sRNAs individually, we wondered whether they could be
351 combined for an additive effect on the riboflavin production. We designed a sRNA array
352 composed of the sRNAs *purR* and *ribDG* each carrying its own promoter and terminator.
353 Combining the two best sRNAs *purR* and *ribDG* increased 10% the riboflavin production
354 compared to only one of them, which represents a 65% increase compared to the
355 parental strain (Figure 5B). Next, we wanted to simultaneously test all the sRNAs
356 developed. To avoid promoter and terminator repetition, we constructed a sRNA operon
357 under control of a single promoter and terminator. The ribozymes RiboJ, RiboJ10,
358 RiboJ60 e RiboJ64 (Nielsen et al., 2016) were inserted in between the sRNAs to promote
359 the release of each sRNA after transcription. The sRNA operon was first tested in the
360 riboflavin super-producing strain (BsRF) resulting in a 44% increase in the riboflavin titer
361 compared to the parental strain (Figure 5B). Although functional, the sRNA operon
362 showed a smaller effect than the best sRNAs individually, which may be attributed to a
363 combination of the positive influence of some sRNAs (*xpt*, *purR*, and *ribDG*) and the
364 negative influence of others (*purE* and *pbuE*) in the riboflavin biosynthesis. Noteworthy,
365 both strains, the BsRF::*purR*-sRNA-*ribDG*-sRNA and the BsRF::*sRNA*-operon, grew to
366 higher culture densities than the parental strain BsRF, closely reproducing the effect
367 observed for the individual sRNAs *ribDG* and *purR*.

368 The BsRF strain has several mutations that increase flux through the riboflavin
369 biosynthetic pathway and increase the availability of the precursor ribulose 6-phosphate.

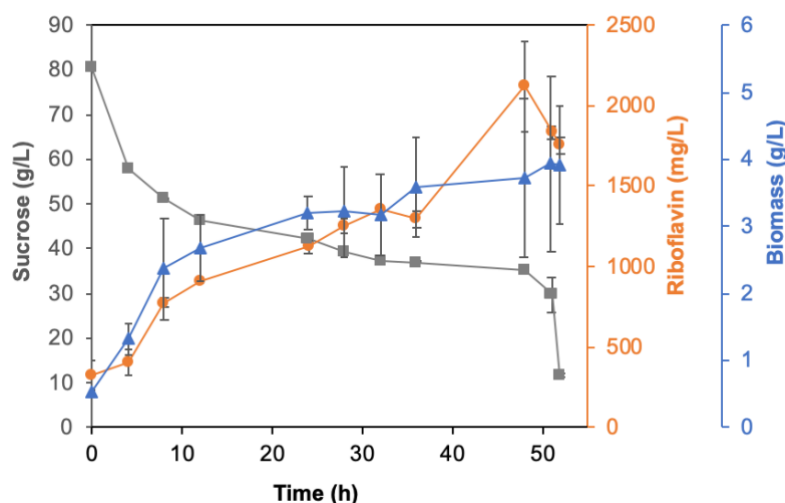
370 Therefore, we hypothesized that the sRNAs effect could be restricted in such a context.
371 In order to evaluate the full potential of the sRNA operon, we inserted it into the genome
372 of a *B. subtilis* strain (BsAi) that carries an extra copy of the riboflavin biosynthetic operon
373 under control of an autoinduction device (Correa et al., 2020), but no other modification.
374 The sRNA operon increased 5-fold the riboflavin production compared to the parental
375 strain (Figure 5C). This result demonstrates that our synthetic sRNA operon is fully
376 functional and capable of targeting gene expression.

377

378 **3.6. The *BsRF::ribDG*-sRNA strain is stable and highly productive in a** 379 **bioreactor scale**

380 In order to demonstrate that our approach is suitable for engineering industrial
381 metabolite-producing strains that are stable and highly productive in large scale, we
382 scaled up the cultivation to a bioreactor. Therefore, one of our best riboflavin producing
383 strain, the *BsRF::ribDG*-sRNA, was cultivated in a 5L batch to access its potential for
384 large scale riboflavin production. The bioreactor was operated in four different conditions
385 regarding the agitation (from 200 to 800 rpm) and the best condition was repeated to
386 confirm the results. Results show that slowing down the rotation to 300 rpm favors
387 riboflavin production over biomass formation (Table S4). Cultivation at this condition
388 resulted in 2.1 g/L of riboflavin after 48h (Figure 6), corresponding to a yield of 44.2 ± 5.9
389 mg/L.h. The final riboflavin titer was 2.2-fold higher compared to the same strain
390 cultivated in Erlenmeyer scale. This result shows that the sRNA-carrying strain is suitable
391 for riboflavin production in large scale.

392



393

394 **Figure 6.** The BsRF::*ribDG*-sRNA strain is stable and highly productive in a bioreactor scale. A
395 5L-batch was carried out for 52h at 300 rpm, 0,5 vvm air supply, and pH controlled at 7.0 ± 0.1 .
396 Samples were withdrawn periodically for sucrose (gray squares), riboflavin (orange circles), and
397 biomass (blue triangles) quantification. Data are presented as mean \pm SD (n = 2). Raw data
398 available in Supplementary Data 3.

399

400 4. Discussion

401 Previously underestimated, RNA has emerged in the last decade as a versatile tool to
402 engineer strains and regulatory circuits (Chappell et al., 2015b; Kelly et al., 2018; Leistra
403 et al., 2019; McCarty et al., 2020). When it comes to regulating gene expression, sRNA
404 stands up as an efficient and easy-to-engineer tool. It has been intensely used to
405 engineer bacteria for gene knockdown by preventing translation initiation (Hoynes-
406 O'Connor and Moon, 2016; Liu et al., 2014; Na et al., 2013; Noh et al., 2017; Yang et al.,
407 2019). Activation of gene expression has been achieved by engineering two RNA
408 molecules, the sRNA and a toehold switch (for translation initiation control) or a Sense
409 target RNA (for transcription termination control) (Chappell et al., 2015a; Green et al.,
410 2014). Our strategy differs from the latter by targeting intrinsic regulatory RNAs
411 (riboswitches) with synthetic sRNAs to activate gene expression.

412 Synthetic sRNAs had been previously designed to target the riboswitches *metH*, *xpt*, and
413 *pbuE*. The sRNAs targeting the *metH* and *xpt* riboswitches completely failed, and the

414 sRNA targeting the *pbuE* riboswitch only activated gene expression by 3.1-fold (Chappell
415 et al., 2015a). Further improvement of the *pbuE* sRNA elevated the activation to 13.4-
416 fold (Meyer et al., 2016). We have successfully designed sRNAs targeting both the *xpt*
417 and the *pbuE* riboswitches. Our *pbuE*-sRNA displays a 103-fold gene activation, which
418 is much higher than achieved by others. Differently from others, our sRNA works as
419 single genome copy. Using genome integrated sRNA genes, instead of plasmid-borne,
420 favors strain stability for engineering metabolite producers suitable for large scale
421 cultivation.

422 We used the riboswitch-targeting sRNAs to engineer a riboflavin-producing strain. The
423 resulting strains were able to reach 50% increase in the riboflavin titer using one sRNA
424 and 65% increase using two sRNAs. Targeting riboswitches with sRNAs seems more
425 efficient than permanent edition. Recently, the *ribDG* riboswitch and the *purR* gene have
426 been edited through CRISPR-Cas9 with the same goal of engineering a riboflavin-
427 producing strain. The engineered strain produced 44% more riboflavin than the parental
428 one (Boumezbeur et al., 2020). Interestingly, the study reports a similar improvement in
429 culture density as observed here. Achieving similar growth improvements using different
430 tools indicates that there are non-anticipated growth-limiting levels of gene expression
431 within the purine and riboflavin pathways that have been alleviated by both approaches.
432 We have developed a new synthetic sRNA tool that targets bacterial riboswitches and
433 activates gene expression at the transcription level. The tool has been validated *in vitro*
434 and *in vivo* against different targets demonstrating specificity. Furthermore, we used the
435 riboswitch-targeting sRNAs to efficiently engineer a riboflavin-producing strain. Finally,
436 we developed an easy-to-engineer multiplex sRNA to target up to five different genes
437 simultaneously. Multiplex sRNA overcomes the obstacles faced by protein-based
438 multiplex control. The tools we developed are broadly applicable to bacterial
439 riboswitches, and are useful to modulate expression of essential genes that cannot be
440 knocked out.

441

442 **Acknowledgements**

443 This work was supported by the São Paulo Research Foundation (FAPESP) [grant
444 2014/17564-7 and 2020/08699-7]; Conselho Nacional de Desenvolvimento Científico e
445 Tecnológico (CNPq) [grant 290110/2017-3 and INCT BioSyn]; and Coordenação de
446 Aperfeiçoamento de Pessoal de Nível Superior - Brasil (CAPES) [Finance Code 001].

447

448 **Supplementary files**

449 Supplementary material

450

451 **Mendeley data**

452 <https://data.mendeley.com/datasets/84yybmrtsx/1>

453 DOI: 10.17632/84yybmrtsx.1

454 Supplementary data 1

455 Supplementary data 2

456 Supplementary data 3

457

458

459 **References**

- 460 Bacher, A., Eisenreich, W., Kis, K., Ladenstein, R., Richter, G., Scheuring, J.,
461 Weinkauff, S., 1993. Biosynthesis of Flavins, in: Dugas, H., Schmidtchen, F.P.
462 (Eds.), *Bioorganic Chemistry Frontiers*. Springer Berlin Heidelberg, Berlin,
463 Heidelberg, pp. 147–192. https://doi.org/10.1007/978-3-642-78110-0_5
- 464 Boumezbeur, A.H., Bruer, M., Stoecklin, G., Mack, M., 2020. Rational engineering of
465 transcriptional riboswitches leads to enhanced metabolite levels in *Bacillus*
466 *subtilis*. *Metab Eng* 61, 58–68. <https://doi.org/10.1016/j.ymben.2020.05.002>
- 467 Chappell, J., Takahashi, M.K., Lucks, J.B., 2015a. Creating small transcription
468 activating RNAs. *Nat Chem Biol* 11, 214–220.
469 <https://doi.org/10.1038/nchembio.1737>
- 470 Chappell, J., Watters, K.E., Takahashi, M.K., Lucks, J.B., 2015b. A renaissance in RNA
471 synthetic biology: new mechanisms, applications and tools for the future. *Curr*
472 *Opin Chem Biol* 28, 47–56.
473 <https://doi.org/https://doi.org/10.1016/j.cbpa.2015.05.018>
- 474 Christiansen, L.C., Schou, S., Nygaard, P., Saxild, H.H., 1997. Xanthine metabolism in
475 *Bacillus subtilis*: characterization of the xpt-pbuX operon and evidence for purine-
476 and nitrogen-controlled expression of genes involved in xanthine salvage and
477 catabolism. *J Bacteriol* 179, 2540–2550. [https://doi.org/10.1128/jb.179.8.2540-](https://doi.org/10.1128/jb.179.8.2540-2550.1997)
478 [2550.1997](https://doi.org/10.1128/jb.179.8.2540-2550.1997)
- 479 Correa, G.G., Lins, M.R.C.R., Silva, B.F., de Paiva, G.B., Zocca, V.F.B., Ribeiro, N.V.,
480 Picheli, F.P., Mack, M., Pedrolli, D.B., 2020. A modular autoinduction device for
481 control of gene expression in *Bacillus subtilis*. *Metab Eng*.
482 <https://doi.org/10.1016/j.ymben.2020.03.012>
- 483 Filonov, G.S., Moon, J.D., Svensen, N., Jaffrey, S.R., 2014. Broccoli: rapid selection of
484 an RNA mimic of green fluorescent protein by fluorescence-based selection and
485 directed evolution. *J Am Chem Soc* 136, 16299–16308.
486 <https://doi.org/10.1021/ja508478x>

- 487 Green, A.A., Silver, P.A., Collins, J.J., Yin, P., 2014. Toehold switches: de-novo-
488 designed regulators of gene expression. *Cell* 159, 925–939.
489 <https://doi.org/10.1016/j.cell.2014.10.002>
- 490 Hoynes-O'Connor, A., Moon, T.S., 2016. Development of Design Rules for Reliable
491 Antisense RNA Behavior in *E. coli*. *ACS Synth Biol* 5, 1441–1454.
492 <https://doi.org/10.1021/acssynbio.6b00036>
- 493 Johansen, L.E., Nygaard, P., Lassen, C., Agerso, Y., Saxild, H.H., 2003. Definition of a
494 Second *Bacillus subtilis* pur Regulon Comprising the pur and xpt-pbuX Operons
495 plus pbuG, nupG (yxjA), and pbuE (ydhL). *J Bacteriol* 185, 5200–5209.
496 <https://doi.org/10.1128/jb.185.17.5200-5209.2003>
- 497 Kalvari, I., Nawrocki, E.P., Ontiveros-Palacios, N., Argasinska, J., Lamkiewicz, K.,
498 Marz, M., Griffiths-Jones, S., Toffano-Nioche, C., Gautheret, D., Weinberg, Z.,
499 Rivas, E., Eddy, S.R., Finn, R.D., Bateman, A., Petrov, A.I., 2021. Rfam 14:
500 expanded coverage of metagenomic, viral and microRNA families. *Nucleic Acids*
501 *Res* 49, D192–D200. <https://doi.org/10.1093/nar/gkaa1047>
- 502 Kelly, C.L., Harris, A.W.K., Steel, H., Hancock, E.J., Heap, J.T., Papachristodoulou, A.,
503 2018. Synthetic negative feedback circuits using engineered small RNAs. *Nucleic*
504 *Acids Res* 46, 9875–9889. <https://doi.org/10.1093/nar/gky828>
- 505 Leistra, A.N., Curtis, N.C., Contreras, L.M., 2019. Regulatory non-coding sRNAs in
506 bacterial metabolic pathway engineering. *Metab Eng* 52, 190–214.
507 <https://doi.org/https://doi.org/10.1016/j.ymben.2018.11.013>
- 508 Lins, M.R.C.R., Correa, G.G., Amorim, L.A.S., Franco, R.A.L., Ribeiro, N.V., de Jesus,
509 V.N., Pedrolli, D.B., 2021. Characterization of five purine riboswitches in cellular
510 and cell-free expression systems. *bioRxiv* 2021.04.14.439898.
511 <https://doi.org/10.1101/2021.04.14.439898>
- 512 Liu, Y., Zhu, Y., Li, J., Shin, H., Chen, R.R., Du, G., Liu, L., Chen, J., 2014. Modular
513 pathway engineering of *Bacillus subtilis* for improved N-acetylglucosamine
514 production. *Metab Eng* 23, 42–52.

- 515 <https://doi.org/https://doi.org/10.1016/j.ymben.2014.02.005>
- 516 Lou, C., Stanton, B., Chen, Y.-J., Munsky, B., Voigt, C.A., 2012. Ribozyme-based
517 insulator parts buffer synthetic circuits from genetic context. *Nat Biotechnol* 30,
518 1137. <https://doi.org/10.1038/nbt.2401>
519 <https://www.nature.com/articles/nbt.2401#supplementary-information>
- 520 Mandal, M., Boese, B., Barrick, J.E., Winkler, W.C., Breaker, R.R., 2003. Riboswitches
521 control fundamental biochemical pathways in *Bacillus subtilis* and other bacteria.
522 *Cell* 113, 577–586.
- 523 Mandal, M., Breaker, R.R., 2004. Gene regulation by riboswitches. *Nat Rev Mol Cell*
524 *Biol* 5, 451–463. <https://doi.org/10.1038/nrm1403>
- 525 Marcano-Velázquez, J.G., Batey, R.T., 2015. Structure-guided mutational analysis of
526 gene regulation by the *Bacillus subtilis* pbuE adenine-responsive riboswitch in a
527 cellular context. *J Biol Chem* 290, 4464–4475.
528 <https://doi.org/10.1074/jbc.M114.613497>
- 529 Mars, R.A.T., Nicolas, P., Denham, E.L., van Dijl, J.M., 2016. Regulatory RNAs in
530 *Bacillus subtilis*: a Gram-Positive Perspective on Bacterial RNA-Mediated
531 Regulation of Gene Expression. *Microbiol Mol Biol Rev* 80, 1029 LP – 1057.
532 <https://doi.org/10.1128/MMBR.00026-16>
- 533 McCarty, N.S., Graham, A.E., Studená, L., Ledesma-Amaro, R., 2020. Multiplexed
534 CRISPR technologies for gene editing and transcriptional regulation. *Nat Commun*
535 11, 1–13. <https://doi.org/10.1038/s41467-020-15053-x>
- 536 Meyer, S., Chappell, J., Sankar, S., Chew, R., Lucks, J.B., 2016. Improving fold
537 activation of small transcription activating RNAs (STARs) with rational RNA
538 engineering strategies. *Biotechnol Bioeng* 113, 216–225.
539 <https://doi.org/https://doi.org/10.1002/bit.25693>
- 540 Mironov, A.S., Gusarov, I., Rafikov, R., Lopez, L.E., Shatalin, K., Kreneva, R.A.,
541 Perumov, D.A., Nudler, E., 2002. Sensing Small Molecules by Nascent RNA: A
542 Mechanism to Control Transcription in Bacteria. *Cell* 111, 747–756.

- 543 [https://doi.org/10.1016/s0092-8674\(02\)01134-0](https://doi.org/10.1016/s0092-8674(02)01134-0)
- 544 Na, D., Yoo, S.M., Chung, H., Park, H., Park, J.H., Lee, S.Y., 2013. Metabolic
545 engineering of *Escherichia coli* using synthetic small regulatory RNAs. *Nat*
546 *Biotechnol* 31, 170–174. <https://doi.org/10.1038/nbt.2461>
- 547 Nielsen, A.A.K., Der, B.S., Shin, J., Vaidyanathan, P., Paralanov, V., Strychalski, E.A.,
548 Ross, D., Densmore, D., Voigt, C.A., 2016. Genetic circuit design automation.
549 *Science* (80-) 352, aac7341. <https://doi.org/10.1126/science.aac7341>
- 550 Noh, M., Yoo, S.M., Kim, W.J., Lee, S.Y., 2017. Gene Expression Knockdown by
551 Modulating Synthetic Small RNA Expression in *Escherichia coli*. *Cell*
552 *Syst* 5, 418-426.e4. <https://doi.org/10.1016/j.cels.2017.08.016>
- 553 Pedrolli, D., Langer, S., Hobl, B., Schwarz, J., Hashimoto, M., Mack, M., 2015. The ribB
554 FMN riboswitch from *Escherichia coli* operates at the transcriptional and
555 translational level and regulates riboflavin biosynthesis. *FEBS J* 282.
556 <https://doi.org/10.1111/febs.13226>
- 557 Pedrolli, D.B., Matern, A., Wang, J., Ester, M., Siedler, K., Breaker, R., Mack, M.,
558 2012. A highly specialized flavin mononucleotide riboswitch responds differently to
559 similar ligands and confers roseoflavin resistance to *Streptomyces davawensis*.
560 *Nucleic Acids Res* 40. <https://doi.org/10.1093/nar/gks616>
- 561 Radeck, J., Kraft, K., Bartels, J., Cikovic, T., Durr, F., Emenegger, J., Kelterborn, S.,
562 Sauer, C., Fritz, G., Gebhard, S., Mascher, T., 2013. The *Bacillus* BioBrick Box:
563 generation and evaluation of essential genetic building blocks for standardized
564 work with *Bacillus subtilis*. *J Biol Eng* 7, 29. [https://doi.org/10.1186/1754-1611-7-](https://doi.org/10.1186/1754-1611-7-29)
565 29
- 566 Richardson, S.M., Wheelan, S.J., Yarrington, R.M., Boeke, J.D., 2006. GeneDesign:
567 rapid, automated design of multikilobase synthetic genes. *Genome Res* 16, 550–
568 556. <https://doi.org/10.1101/gr.4431306>
- 569 Rodrigo, G., Jaramillo, A., 2014. RiboMaker: computational design of conformation-
570 based riboregulation. *Bioinformatics* 30, 2508–2510.

- 571 <https://doi.org/10.1093/bioinformatics/btu335>
- 572 Rostain, W., Landrain, T.E., Rodrigo, G., Jaramillo, A., 2015. Regulatory RNA design
573 through evolutionary computation and strand displacement. *Methods Mol Biol*
574 1244, 63–78. https://doi.org/10.1007/978-1-4939-1878-2_4
- 575 Rouillard, J.-M., Lee, W., Truan, G., Gao, X., Zhou, X., Gulari, E., 2004. Gene2Oligo:
576 oligonucleotide design for in vitro gene synthesis. *Nucleic Acids Res* 32, W176-80.
577 <https://doi.org/10.1093/nar/gkh401>
- 578 Saxild, H.H., Brunstedt, K., Nielsen, K.I., Jarmer, H., Nygaard, P., 2001. Definition of
579 the *Bacillus subtilis* PurR Operator Using Genetic and Bioinformatic Tools and
580 Expansion of the PurR Regulon with *glyA*, *guaC*, *pbuG*, *xpt-pbuX*, *yqhZ-foID*, and
581 *pbuO*. *J Bacteriol* 183, 6175–6183. [https://doi.org/10.1128/jb.183.21.6175-](https://doi.org/10.1128/jb.183.21.6175-6183.2001)
582 [6183.2001](https://doi.org/10.1128/jb.183.21.6175-6183.2001)
- 583 Shi, T., Wang, Y., Wang, Z., Wang, G., Liu, D., Fu, J., Chen, T., Zhao, X., 2014.
584 Deregulation of purine pathway in *Bacillus subtilis* and its use in riboflavin
585 biosynthesis. *Microb Cell Fact* 13, 101. <https://doi.org/10.1186/s12934-014-0101-8>
- 586 Shimoni, Y., Friedlander, G., Hetzroni, G., Niv, G., Altuvia, S., Biham, O., Margalit, H.,
587 2007. Regulation of gene expression by small non-coding RNAs: a quantitative
588 view. *Mol Syst Biol* 3, 138. [https://doi.org/https://doi.org/10.1038/msb4100181](https://doi.org/10.1038/msb4100181)
- 589 Sun, D., Chen, J., Wang, Y., Li, M., Rao, D., Guo, Y., Chen, N., Zheng, P., Sun, J., Ma,
590 Y., 2019. Metabolic engineering of *Corynebacterium glutamicum* by synthetic
591 small regulatory RNAs. *J Ind Microbiol Biotechnol* 46, 203–208.
592 <https://doi.org/10.1007/s10295-018-02128-4>
- 593 Yang, D., Yoo, S.M., Gu, C., Ryu, J.Y., Lee, J.E., Lee, S.Y., 2019. Expanded synthetic
594 small regulatory RNA expression platforms for rapid and multiplex gene
595 expression knockdown. *Metab Eng* 54, 180–190.
596 [https://doi.org/https://doi.org/10.1016/j.ymben.2019.04.003](https://doi.org/10.1016/j.ymben.2019.04.003)
- 597 Yang, Y., Lin, Y., Li, L., Linhardt, R.J., Yan, Y., 2015. Regulating malonyl-CoA
598 metabolism via synthetic antisense RNAs for enhanced biosynthesis of natural

599 products. *Metab Eng* 29, 217–226.

600 <https://doi.org/https://doi.org/10.1016/j.ymben.2015.03.018>

601 Zadeh, J.N., Steenberg, C.D., Bois, J.S., Wolfe, B.R., Pierce, M.B., Khan, A.R., Dirks,

602 R.M., Pierce, N.A., 2011. NUPACK: Analysis and design of nucleic acid systems.

603 *J Comput Chem* 32, 170–173. <https://doi.org/10.1002/jcc.21596>

604